Icarus 378 (2022) 114947

Contents lists available at ScienceDirect

Icarus

journal homepage: www.elsevier.com/locate/icarus

Partition sums for non-local thermodynamic equilibrium conditions for nine molecules of importance in planetary atmospheres

Robert R. Gamache [a,*], Bastien Vispoel [b,c], Michaël Rey [d], Vladimir Tyuterev [d,e], Alain Barbe [d], Andrei Nikitin [f], Oleg L. Polyansky [g], Jonathan Tennyson [g], Sergei N. Yurchenko [g], Attila G. Császár [h], Tibor Furtenbacher [h], Valery I. Perevalov [f], Sergei A. Tashkun [f]

[a] Department of Environmental, Earth and Atmospheric Sciences, University of Massachusetts Lowell, Lowell, MA 01854, USA
[b] Research Unit Lasers and Spectroscopies (LLS), Institute of Life, Earth and Environment (ILEE), University of Namur (UNamur), 61 rue de Bruxelles, B-5000 Namur, Belgium
[c] Royal Belgian Institute for Space Aeronomy (BIRA-IASB), 3 Avenue Circulaire, 1180 Brussels, Belgium
[d] Groupe de Spectrométrie Moléculaire et Atmosphérique, UMR CNRS 7331, Université de Reims, U.F.R. Sciences, B.P. 1039, 51687 Reims Cedex 2, France
[e] Laboratory of Quantum mechanics and Radiative Processes, Tomsk State University, 36 Lenin avenue, 634050, Russia
[f] Laboratory of Theoretical Spectroscopy, V.E. Zuev Institute of Atmospheric Optics, SB RAS 1, Akademician Zuev Sq., Tomsk 634055, Russian Federation
[g] Department of Physics and Astronomy, University College London, Gower Street, London WC1E 6BT, United Kingdom
[h] ELKH-ELTE Complex Chemical Systems Research Group and Laboratory of Molecular Structure and Dynamics, Institute of Chemistry, ELTE Eötvös Loránd University, Pázmány Péter sétány 1/A, H-1117 Budapest, Hungary

ARTICLE INFO

Keywords:
NLTE
Partition sums
Planetary and exoplanet atmospheres

ABSTRACT

Internal vibrational and rotational partition functions are calculated for nine molecules that are abundant in the terrestrial atmosphere and some are also observed in planetary and exoplanet atmospheres. These molecules are often observed in non-local thermodynamic equilibrium (NLTE) conditions. Calculations are made for all isotopologues of these molecules for which data are available, generally for the temperature range $T = 1$–5000 K. The methods of calculation of the vibrational and rotational partition functions, Q_v and Q_r, respectively, the convergence, and the uncertainties for each isotopologue are discussed. Finally, a FORTRAN program, NLTE_TIPS_2021.FOR, to recall the NLTE partition sums is discussed.

1. Introduction

When studying planetary atmospheres via spectroscopy, the radiative transfer equations are solved by following the radiation as it passes through roughly isothermal-isobaric layers, where at each layer the incoming and outgoing radiations are determined. At each layer, the line intensity and line shape parameters must be determined for the pressure and temperature of the layer based on reference values, which can be found in molecular spectroscopic databases such as HITRAN(Gordon et al., 2021) or GEISA(Delahaye et al., 2021). As long as the pressure and temperature are not too low, the number of collisions per unit time will be sufficient for the populations of the quantum energy states to follow the Boltzmann law and the molecular velocity distribution to remain Maxwellian. This condition is called Local-Thermodynamic Equilibrium (LTE). However, if the conditions change such that the number of collisions per unit time is too low, one finds that the populations deviate from the Boltzmann law while the molecular velocity distribution remains Maxwellian. This occurs whenever collisions between molecules are infrequent enough that the radiative lifetimes of the important vibrational states of a molecule become comparable to the mean time between collisions. This condition is labeled Non-Local Thermodynamic Equilibrium (NLTE).

The change in conditions can be understood by considering the hydrostatic equation, which shows that atmospheric pressure and density decrease exponentially as a function of altitude. Kinetic theory states the collision frequency of a molecule is proportional to the molecule's collisional cross-section, mean speed, and the density; the first two depending on the molecule in question and the latter on the conditions (pressure, temperature, and altitude). Hence, the number of collisions per unit time decreases exponentially as well and there will be an altitude at which the conditions needed to maintain LTE no longer exist. For CO_2 in the Earth's atmosphere the deviation from LTE starts at around

* Corresponding author.
E-mail address: Robert_Gamache@uml.edu (R.R. Gamache).

https://doi.org/10.1016/j.icarus.2022.114947
Received 1 December 2021; Received in revised form 4 February 2022; Accepted 10 February 2022
Available online 15 February 2022
0019-1035/© 2022 Elsevier Inc. All rights reserved.

70 km. At this point, the population of states is not given by the Boltzmann distribution but can be described by NLTE modeling. The population of energy states is crucially important in modeling atmospheres.

Considering the role of CO_2 on the energy budget of Earth's middle atmosphere, the effects of modeling with or without NLTE can be understood straightforwardly. The ν_2 (bending) vibrational band of CO_2 at 15 μm is the dominant source of cooling by transferring radiation to space and the near-IR bands contribute substantially to the heating rate during the day by the absorption of incoming solar radiation. The more (less) the population of states in the 15 μm band means the more(less) radiation transferred to space(cooling / less cooling); the more(less) the population of states in the near-IR bands the more(less) radiation absorbed(heating / less heating). Thus, moving molecules in or out of these states will affect the energy budget of the middle atmosphere. Because the change from LTE to NLTE conditions affects the populations of these states, NLTE modeling must be done in order to obtain the population data and determine the correct energy budget.

Strictly speaking, perfect LTE or NLTE conditions are seldom encountered in planetary atmospheres. As shown by López-Puertas et al. (1990), the atmosphere is in a state that might be called partial LTE, in which the velocity distribution of molecules is Maxwellian but only some groups of levels obey the Boltzmann relation. If one follows a volume of gas and traces its state as the density decreases, then generally one would observe a series of partial LTE states, in which ever fewer levels follow the Boltzmann relation (Kutepov et al., 1998). In conditions of NLTE, collisional energy exchange alone, under conditions of lower atmospheric pressure, no longer determines the internal energy level populations because of the increased importance of radiative and chemical pumping and radiative losses. The partition of population is then characterized by a temperature different from the local kinetic temperature. For these conditions, the solution of the radiative transfer equations is preceded by solving the statistical equilibrium equations (SEE), which consider a large number of excited states of different molecular species coupled by a variety of collisional energy exchange processes and by band overlapping, together with a detailed model of atmospheric stratification.

When solving the radiative transfer equations in conditions of NLTE, the line intensities must be corrected to account for the change in the populations of states. This correction is done using a partition function appropriate for NLTE conditions, as shown by Edwards et al. (1998a). Using these corrections López-Puertas et al. (López-Puertas et al., 1986a; López-Puertas et al., 1986b) studied the 15 μm bands of CO_2 in the middle atmosphere and clearly demonstrated that NLTE corrections were necessary to model heating and cooling rates in the middle atmosphere.

Hummer et al. (Däppen et al., 1988; Hummer and Mihalas, 1988; Mihalas et al., 1988) formulated the equation of state for materials in stellar envelopes at low densities by using an occupation probability formalism that accounts for the perturbations of bound states by both neutral and charged perturbers. The formalism was then applied to the computation of the thermodynamic properties of a partially ionized (and/or dissociated) multicomponent gas. Kutepov et al. (1998) presented a general formulation of the multi-level rotation-vibration NLTE problem for a mixture of radiating molecular gases in a planetary atmosphere, treating explicitly the coupling of molecular energy levels by collisionally-induced energy-transfer processes and by band overlap. More recently, Young et al. (2020) demonstrated that exoplanet upper atmospheres are low-density environments, where radiative processes can compete with collisional ones and introduce NLTE effects into transmission spectra. By adapting the spectral synthesis code Cloudy for NLTE calculations, they produced an atmospheric structure and atomic transmission spectrum in both NLTE and LTE for the hot Jupiter HD209458b. Their results demonstrated that individual spectral lines in the NLTE spectrum exhibit up to 40% stronger absorption that the corresponding lines in the LTE spectra, demonstrating the need for NLTE modeling of spectra (Fossati et al., 2020) as discussed above, recognizing the need to observationally constrain the atmospheric temperature-pressure (TP) profile of exoplanets, developed a data-driven approach to constrain the TP profile of the ultra-hot Jupiter KELT-9b by fitting synthetic spectra to the observed H_α and H_β lines and identified why self-consistent planetary TP models are unable to fit the observations. They constructed 126 one-dimensional TP profiles varying the lower and upper atmospheric temperatures, as well as the location and gradient of the temperature rise. For each profile, transmission spectra were computed accounting for non-local thermodynamic equilibrium effects. Their results demonstrated that the assumption of LTE overestimates the level populations of excited hydrogen by several orders of magnitude, indicating the need for including NLTE effects when modeling exoplanet atmospheres.

Laboratory measurements are also being made to elucidate NLTE effects that are essential for determining the properties of Hot-Jupiter-type exoplanets (Bernath, 2014; Swain et al., 2008; Tinetti et al., 2013). Dudás et al. (2020) have developed a novel approach to produce NLTE IR spectra using a hypersonic expansion probed by cavity ring-down spectroscopy (CRDS). They have used this method to study both the CO and CH_4 molecules and have extracted from the work the rotational and vibrational temperatures necessary to characterize the NLTE.

In this work, the determination of the internal vibrational and rotational partition functions needed for NLTE computations is undertaken for nine molecules that are often observed in NLTE conditions and are abundant in planetary and exoplanet atmospheres: H_2O, CO_2, O_3, N_2O, CO, CH_4, NO, NO_2, and OH. The methods of calculation are reviewed for each molecule/isotopologue. A code, NLTE_TIPS_2021.FOR, that can quickly recall the vibrational NLTE and rotational LTE partition sums is then discussed.

2. Calculations of the vibrational and rotational partition sums

The calculation of the total internal partition sum (TIPS) is discussed for both LTE and NLTE conditions. For LTE, the most accurate TIPS are made by direct summation over very large sets of rovibrational *term values*, which usually come from *first-principles* calculations. However, for many of the molecules in question, these large sets of *term values* are not available, and the product approximation (Gamache et al., 1990; Gamache et al., 2000) must be made. In NLTE applications, the rotational and vibrational partition sums must be determined for a number of layers in the atmosphere. When *first-principles* data are available for the molecules, e.g., for H_2O and CO_2, the calculations of the NLTE partition sums can be made. However, the summing over the energies is time-consuming and must be done for each atmospheric layer since the correct vibrational temperature must be used for each state. Note also that if the atmospheric conditions change, the sums must be redone. A faster approach is to apply the product approximation to determine Q_v and Q_r separately. In this study, the product approximation is used for all the molecules.

2.1. LTE conditions

Under conditions of local thermodynamic equilibrium, the line intensity for a transition from initial state i to final state f at temperature T is given by

$$S_{if}(T) = I_a \frac{A_{if}}{8\pi c \omega_{if}^2} \frac{g_i\, e^{-hcE_i/kT}\left(1 - e^{-hc\,\omega_{if}/kT}\right)}{Q(T)} \quad (1)$$

where I_a is the natural abundance of the isotopologue (note that we are following the HITRAN (Gordon et al., 2021) definition of intensity that includes the isotopic abundance, for other databases that do not include this factor I_a should be set to 1.), A_{if} [s^{-1}] is the Einstein A-coefficient, g_i is the lower state statistical weight, E_i is the energy (*term value*) of state i, (lower state energy in cm^{-1}), h, and k are the Planck and Boltzmann

constants, respectively, c is the speed of light in vacuum, ω_{if} is the wavenumber of the transition, and $Q(T)$ is the total internal partition sum at temperature T. The total internal partition sum is given by a sum over all quantum states of the molecule,

$$Q(T) = \sum_{\substack{\text{all}\\ \text{quantum}\\ \text{states } s}} g_s\, e^{-hcE_s/kT} \tag{2}$$

For the LTE condition, we have the Maxwell−Boltzmann distributions in thermal equilibrium at a temperature T(K), for which the number of molecules [cm^{-3}] in a rovibrational state, n_{vJ}, labeled by v and J, of energy E_{vJ} [cm^{-1}] and of statistical weight g_{vJ} is

$$n_{vJ}(T) = N\,\frac{g_{vJ}\, e^{-hcE_{vJ}/kT}}{Q(T)} \tag{3}$$

where N [molecules cm^{-3}] is the molecular number density. One can write the population probability as

$$W^*_{vJ}(T) = \frac{g_{vJ}\, e^{-hcE_{vJ}/kT}}{Q(T)} \tag{4}$$

with the condition.

$$\sum_{v,J} W^*_{vJ}(T) = 1 \tag{5}$$

In this study, the molecules are in the electronic ground state and rotation and vibration are the only quantized motions, i.e., tunneling, internal rotations, etc. are not considered. Assuming no rotational-vibrational interactions, the wavefunction of the state can be written as a product of the vibrational wavefunction times the rotational wavefunction and the energy is given as a sum of vibrational and rotational energies,

$$E_{vJ} = E_v + E_J \tag{6}$$

Eq. (2) can be rewritten as

$$Q(T) = \sum_{v,J} g_{vJ}\, e^{-hc(E_v+E_J)/kT} = \sum_v g_v\, e^{-hc(E_v)/kT} \times \sum_J g_J\, e^{-hc(E_J)/kT} \tag{7}$$

where $g_{vJ} = g_v g_J$. This is called the product approximation (PA) and TIPS can be written as

$$Q(T) = Q_v(T)\, Q_r(T) \tag{8}$$

where the vibrational partition sum is

$$Q_v(T) = \sum_{\substack{\text{all}\\ \text{vibrational}\\ \text{states}}} g_v\, e^{-hcE_v/kT} \tag{9}$$

and the rotational partition sum is.

$$Q_r(T) = \sum_{\substack{\text{all}\\ \text{rotational}\\ \text{states}}} g_J\, e^{-hcE_J/kT} \tag{10}$$

Population probabilities can be written, similar to Eq. (4), for the vibrational and rotational states.

Using Eq. (3), Eq. (1) can be rewritten as

$$S_{if}(T) = I_a \frac{A_{if}}{8\pi c\,\omega_{if}^2}\,\frac{n_i(T)}{N}\left(1 - e^{-hc\omega_{if}/kT}\right) \tag{11}$$

Note that in most cases the induced emission (IE) term in Eqs. (1) or (11), $\left(1 - e^{-hc\omega_{if}/kT}\right)$, is approximately one. At 296 K the IE term for the 183 GHz (6.104 cm^{-1}) line of H_2O is 0.0302, however, for an IR transition, say at 2000 cm^{-1}, the IE term is 0.99996. The same terms at 1000 K are 0.009 and 0.9490, respectively. So, often the IE term can be neglected when the wavenumber of the transition is in the infrared or higher.

2.2. NLTE conditions

As noted first in the introduction, a gas can be said to be in a state of NLTE when the population of the levels deviate from the Boltzmann law while the molecular velocity distribution remains Maxwellian. The translational, rotational, and vibrational levels of a molecular system adjust to equilibrium at very different rates. As a consequence, for most of the atmospheric species in the upper atmosphere, the translational and rotational levels are in LTE, while the vibrational ones are not. For such conditions, the populations of the states are no longer determined by simple Boltzmann statistics, but rather by a mixture of collisional reactions and exchange of vibrational quanta. The former can involve both vibrational-thermal and vibrational-vibrational exchanges, and both can involve a multiplicity of levels and exchange partners. Edwards et al. (1998b) has shown that this state can be described with a similar probability formalism as LTE by introducing at each point a set of vibrational temperatures, T_ν, in place of the kinetic temperature, T. The vibrational temperatures are defined by the vibrational level populations determined by the SEE models. The model includes vibrational-thermal (V-T) and vibrational-vibrational (V—V) collisional processes, absorption of solar radiation, exchange of photons between atmospheric layers, and spontaneous emission (for details see Edwards et al., 1998 and references therein). Once these populations are known, the vibrational temperature for the vibrational state labeled j is defined with reference to the ground state (subscript 0)

$$T_{\nu_j} = \frac{hcE_{\nu_j}}{kln\left(\frac{g_{\nu_j}}{g_0}\frac{n_0}{\tilde{n}_{\nu_j}}\right)} \tag{12}$$

where $E_{\nu j}$, $\tilde{n}_{\nu_j}$, $g_{\nu j}$, are the energy, number of molecules in, and statistical weight of the vibrational state j, n_0 and g_0 are the number of molecules in and statistical weight of the ground vibrational state.

Eq. (8) can still be used to determine the rotational partition sum, $Q_r(T)$, since the rotational states are still in LTE. Because the vibrational levels are in NLTE, the usual expression for the vibrational partition sum, see for example Herzberg's harmonic approximation (HA) (Herzberg, 1960) or including anharmonic corrections to the vibrational levels (Gamache et al., 2017), cannot be used. $Q_v(T)$ in Eq. (9) must now be determined via a direct sum, where the appropriate vibrational temperatures must be used. Rewriting Eq. (9) as

$$\tilde{Q}_v(T) = \sum_{v_j=1}^{v_{max}} g_{v_j}\, e^{-hcE_{v_j}/kT_{v_j}} \tag{13}$$

where the tilde labels a NLTE quantity, T is the kinetic temperature and $T_{\nu j}$ is the vibrational temperature for state ν_j. The sum goes up to some maximum vibrational level, ν_{max}, that ensures convergence of the sum. Due to the advent of extensive *first-principles* calculations, the set of ν_js are known for many molecules. The $T_{\nu j}$ are determined for each vibrational state by chemical-dynamical models (see Edwards et al., 1993; Edwards et al., 1998; López-Puertas et al., 1990; López-Puertas et al., 1986a; López-Puertas et al., 1986b). It should be noted that many vibrational states are not involved in the chemistry and dynamics that shifts population, so for these states, $T_{\nu j}$ is the kinetic temperature.

2.3. The non-LTE correction to the line intensity

Under conditions of LTE, radiative transfer theory for the two levels of a transition defines a spectral line intensity in terms of the Einstein-B coefficient for absorption for a transition $f \leftarrow i$ as (Gamache and

Rothman, 1992)

$$S_{if} = \frac{h\omega_{if}}{c} B_{if} n_i \left(1 - \frac{g_i n_f}{g_f n_i}\right) \quad (14)$$

where B_{if} is the Einstein coefficient for absorption, n_i and n_f are the populations of the lower and upper states, respectively, g_i and g_f are the level statistical weights of the lower and upper states, respectively, and ω_{if} the transition wavenumber.

The ratio of the populations of the upper and lower levels,

$$\frac{n_f}{n_i} = \frac{\left(N g_f e^{-hcE_f/kT_{kin}}\right)/Q}{\left(N g_i e^{-hcE_i/kT_{kin}}\right)/Q} = \frac{g_f}{g_i} exp\left(-hc\left(E_f - E_i\right)/kT_{kin}\right) = \frac{g_f}{g_i} exp\left(-hc\omega_{if}/kT_{kin}\right) \quad (15)$$

can be rearranged to give the last factor in the parentheses in Eq. (14), which is designated as the Boltzmann factor Γ at the local kinetic temperature T_{kin},

$$\Gamma = \frac{g_i n_f}{g_f n_i} = exp\left(-hc\omega_{if}/kT_{kin}\right) \quad (16)$$

The line intensity can be rewritten, where the quantities that depend on temperature are explicitly noted,

$$S_{if}(T_{kin}) = \frac{h\omega_{if}}{c} B_{if} n_i(T_{kin}) \left(1 - e^{-hc\omega_{if}/kT_{kin}}\right) \quad (17)$$

In LTE, $T_{kin} = T$ and given data at a reference temperature, T_{ref}, the temperature at another T can be obtained by taking the ratio of Eq. (17) expressed at the two temperatures.

$$S_{if}(T) = S_{if}(T_{ref}) \frac{n_i(T)\left(1 - e^{-hc\omega_{if}/kT}\right)}{n_i(T_{ref})\left(1 - e^{-hc\omega_{if}/kT_{ref}}\right)} = S_{if}(T_{ref}) \frac{g_i e^{-hcE_i/kT}/Q(T)\left(1 - e^{-hc\omega_{if}/kT}\right)}{g_i e^{-hcE_i/kT_{ref}}/Q(T_{ref})\left(1 - e^{-hc\omega_{if}/kT_{ref}}\right)} \quad (18)$$

Cancelling like terms and assuming $E = E_v + E_r$ to obtain the product approximation, $Q(T) = Q_v(T)\,Q_r(T)$ gives.

$$S_{if}(T) = S_{if}(T_{ref}) \frac{Q_v(T_{ref})\,Q_r(T_{ref})}{Q_v(T)\,Q_r(T)} e^{-hcE_i/k\left(\frac{1}{T} - \frac{1}{T_{ref}}\right)} \left(\frac{1 - e^{-hc\omega_{if}/kT}}{1 - e^{-hc\omega_{if}/kT_{ref}}}\right) \quad (19)$$

Writing Eq. (15) for the NLTE case and using a tilde to signify quantities in NLTE gives.

$$\frac{\widetilde{n}_f}{\widetilde{n}_i} = \frac{\left(N g_f e^{-hcE_f/kT^*}\right)/\widetilde{Q}}{\left(N g_i e^{-hcE_i/kT_{kin}}\right)/\widetilde{Q}} \quad (20)$$

where T^* signifies that the vibrational and rotational temperatures may be different. Note, it was assumed that for the lower level, i, the vibrational and rotational temperatures are the same. If it is not the case, the equation must be modified.

Allowing for the final state to have different vibrational and rotational temperatures gives $E_f = E_v(T_v) + E_r(T_{kin})$ and the ratio of populations is

$$\frac{\widetilde{n}_f}{\widetilde{n}_i} = \frac{g_f e^{-hcE_{v_f}/kT_v} e^{-hcE_{r_f}/kT_{kin}}}{g_i e^{-hcE_i/kT_{kin}}} \quad (21)$$

The line intensity for the NLTE case is.

$$\widetilde{S}_{if}(T_{kin}) = \frac{h\omega_{if}}{c} B_{if} \widetilde{n}_i(T_{kin}) \left(1 - \frac{e^{-hcE_{v_f}/kT_v} e^{-hcE_{r_f}/kT_{kin}}}{e^{-hcE_i/kT_{kin}}}\right) \quad (22)$$

Using Eqs. (17) and (22), the NLTE intensity at some kinetic temperature can be written in terms of the LTE intensity (scaled to T_{kin} from HITRAN).

$$\widetilde{S}_{if}(T_{kin}) = S_{if}(T_{kin}) \frac{\widetilde{n}_i(T_{kin})}{n_i(T_{kin})} \frac{\left(1 - \frac{e^{-hcE_{v_f}/kT_v} e^{-hcE_{r_f}/kT_{kin}}}{e^{-hcE_i/kT_{kin}}}\right)}{\left(1 - e^{-hc\omega_{if}/kT_{kin}}\right)} \quad (23)$$

Noting that $\widetilde{n}_i(T) = N \frac{g_i e^{-hcE_i/kT}}{\widetilde{Q}(T)}$, where again we have assumed that in the lower state the vibrational and rotational temperatures are the same. Thus, the ratio of the population of state i in NLTE to LTE is the inverse ratio of the partition sums; $\widetilde{Q}$ is written as $\widetilde{Q}_v\ Q_r$, giving

$$\widetilde{S}_{if}(T_{kin}) = S_{if}(T_{kin}) \frac{Q(T_{kin})}{\widetilde{Q}_v(T_v)\ Q_r(T_{kin})} \frac{\left(1 - \frac{e^{-hcE_{v_f}/kT_v} e^{-hcE_{r_f}/kT_{kin}}}{e^{-hcE_i/kT_{kin}}}\right)}{\left(1 - e^{-hc\omega_{if}/kT_{kin}}\right)} \quad (24)$$

where $\widetilde{Q}_v$ is evaluated using Eq. (13) and it should be noted that the determination of $\widetilde{Q}_v$ allows for a different value of T_v for each vibrational level. The NLTE line intensity can also be written in terms of the HITRAN line intensity at the reference temperature.

$$\widetilde{S}_{if}(T_{kin}) = S_{if}(T_{ref}) \frac{Q_v(T_{ref})\,Q_r(T_{ref})}{\widetilde{Q}_v(T_v)\,Q_r(T_{kin})} e^{-hcE_i/k\left(\frac{1}{T_{kin}} - \frac{1}{T_{ref}}\right)} \frac{\left(1 - \frac{e^{-hcE_{v_f}/kT_v} e^{-hcE_{r_f}/kT_{kin}}}{e^{-hcE_i/kT_{kin}}}\right)}{\left(1 - e^{-hc\omega_{if}/kT_{ref}}\right)} \quad (25)$$

Table 1
Isotopologue, maximum rotational *term value*, maximum vibrational *term value,* number of vibrational states, maximum temperature of reported partition sums.

Molecular Isotopologue	Maximum rotational *term value* cm^{-1}	RC[a] at T_{max}	Maximum $G(\nu_1, \nu_2, \nu_3)$ cm^{-1}	VC[b] at T_{max}	# vibrational states	T_{max} (K)
$H_2{}^{16}O$	36,841.5	0.34	41,121.6	0.27	464	5000
$H_2{}^{18}O$	36,841.5	0.34	41,880.9	0.05	1098	5000
$H_2{}^{17}O$	36,841.5	0.34	41,913.6	0.05	1100	5000
$HD^{16}O$	25,156.8	1.08	29,665.8	0.10	600	4000
$HD^{18}O$	25,156.8	1.08	32,449.2	0.05	800	4000
$HD^{17}O$	25,156.8	1.08	32,511.4	0.05	800	4000
$D_2{}^{16}O$	11,363.0	1.93	41,998.1	0.00	2819	2000
$D_2{}^{18}O$	11,386.9	1.85	41,985.5	0.00	2848	2000
$D_2{}^{17}O$	11,377.6	1.88	41,992.6	0.00	2835	2000
$^{12}C^{16}O_2$	19,747.5	0.48	24,000.0	0.14	8325	3000
$^{13}C^{16}O_2$	19,747.2	0.48	23,997.7	0.14	8998	3000
$^{16}O\ ^{12}C^{18}O$	18,649.5	0.62	23,999.9	0.14	8747	3000
$^{16}O\ ^{12}C^{17}O$	19,169.8	0.54	23,998.8	0.14	9444	3000
$^{16}O\ ^{13}C^{18}O$	18,648.6	0.62	23,998.1	0.14	8530	3000
$^{16}O\ ^{13}C^{17}O$	19,170.2	0.54	23,999.7	0.14	9217	3000
$^{12}C^{18}O_2$	17,582.8	0.86	23,999.8	0.14	9132	3000
$^{18}O\ ^{12}C^{17}O$	18,088.1	0.73	23,999.5	0.14	8951	3000
$^{12}C^{17}O_2$	18,600.2	0.63	23,999.7	0.14	8745	3000
$^{13}C^{18}O_2$	17,582.8	0.86	23,999.6	0.15	9901	3000
$^{18}O\ ^{13}C^{17}O$	18,088.2	0.73	23,999.9	0.15	9667	3000
$^{13}C^{17}O_2$	18,600.7	0.63	23,999.1	0.14	9450	3000
$^{16}O_3$	NA[c]	–	25,615.4	0.00	1000	1000
$^{16}O^{16}O^{18}O$	NA	–	25,227.7	0.00	1000	1000
$^{16}O^{18}O^{16}O$	NA	–	24,984.6	0.00	1000	1000
$^{16}O^{16}O^{17}O$	NA	–	25,411.4	0.00	1000	1000
$^{16}O^{17}O^{16}O$	NA	–	25,283.7	0.00	1000	1000
$^{18}O^{18}O^{16}O$	NA	–	24,589.2	0.00	1000	1000
$^{18}O^{16}O^{18}O$	NA	–	24,836.9	0.00	1000	1000
$^{16}O^{17}O^{18}O$	NA	–	24,891.6	0.00	1000	1000
$^{17}O^{16}O^{18}O$	NA	–	25,021.8	0.00	1000	1000
$^{17}O^{18}O^{16}O$	NA	–	24,773.1	0.00	1000	1000
$^{17}O^{17}O^{16}O$	NA	–	25,078.8	0.00	1000	1000
$^{17}O^{16}O^{17}O$	NA	–	25,209.0	0.00	1000	1000
$^{18}O^{18}O^{18}O$	NA	–	24,190.8	0.00	1000	1000
$^{18}O^{18}O^{17}O$	NA	–	24,369.8	0.00	1000	1000
$^{18}O^{17}O^{18}O$	NA	–	24,488.1	0.00	1000	1000
$^{17}O^{17}O^{18}O$	NA	–	24,679.3	0.00	1000	1000
$^{17}O^{18}O^{17}O$	NA	–	24,560.0	0.00	1000	1000
$^{17}O^{17}O^{17}O$	NA	–	24,869.8	0.00	1000	1000
$^{14}N^{14}N^{16}O$	NA	–	32,579.7	0.59	3000	5000
$^{14}N^{15}N^{16}O$	NA	–	31,883.3	0.65	3000	5000
$^{15}N^{14}N^{16}O$	NA	–	32,119.2	0.63	3000	5000
$^{14}N^{14}N^{18}O$	NA	–	32,093.0	0.62	3000	5000
$^{14}N^{14}N^{17}O$	NA	–	32,266.7	0.61	3000	5000
$^{12}C^{16}O$	39,966.3	0.14	66,960.7	0.00	42	5000
$^{12}C^{18}O$	38,197.9	0.18	65,930.1	0.00	42	5000
$^{12}C^{17}O$	39,029.8	0.19	65,843.0	0.00	42	5000
$^{13}C^{16}O$	38,333.4	0.16	66,374.2	0.00	42	5000
$^{13}C^{18}O$	36,552.4	0.24	64,763.0	0.00	42	5000
$^{13}C^{17}O$	37,390.3	0.21	65,317.8	0.00	42	5000
$^{14}C^{16}O$	36,929.7	0.23	65,014.1	0.00	42	5000
$^{14}C^{18}O$	35,137.9	0.31	63,802.0	0.00	42	5000
$^{14}C^{17}O$	35,980.9	0.27	64,378.4	0.00	42	5000
$^{12}CH_4$	30,424.1	0.37	134,152.1	0.22	493,869	5000
$^{13}CH_4$	NA	–	133,446.7	0.23	493,869	5000
$^{12}CH_3D$	NA	–	68,870.9	1.73	272,781	5000
$^{13}CH_3D$	NA	–	68,560.2	1.75	272,781	5000
$^{14}N^{16}O$	35,512.0	0.27	28,139.6	0.14	16	5000
$^{15}N^{16}O$	34,354.3	0.36	27,409.3	0.16	16	5000
$^{14}N^{18}O$	33,814.0	0.33	27,643.8	0.15	16	5000
$^{14}N^{16}O_2$	NA	–	33,183.0	0.68	1000	5000
$^{15}N^{16}O_2$	NA	–	32,657.0	0.73	1000	5000
^{16}OH	66,754.3	0.00	33,086.4	0.04	14	5000
^{18}OH	39,691.4	0.00	31,585.6	0.10	13	5000
^{16}OD	42,953.3	0.00	32,642.9	0.08	13	5000

[a] convergence of Q_{rot} in percent; see text.
[b] convergence of Q_{vib} in percent; see text.
[c] analytical formula used.

3. Calculations of Q_r and Q_v

The calculations of the rotational and vibrational partition sums are presented for each molecule/isotopologue of this study. In all the calculations, *h*, *k*, and *c*, are the 2014 CODATA values (Mohr et al., 2016). Note, the Q_vs determined below are the LTE values and were used to check the calculations by comparing with the TIPS2017 values (Gamache et al., 2017). The algorithm discussed in section 4 provides the NLTE Q_v.

To apply Eq. (13) to determine $\widetilde{Q}_v(T)$, files of the vibrational term

Table 2
Term value versus maximum temperature for convergence of vibrational partition sum. Note that this table excludes methane.

Maximum term value in cm^{-1}	Maximum temperature (K) of converged Q_{vib}
5000.	500
8000.	1000
10,000.	1500
14,000.	2000
21,000.	3000
32,000.	4000
37,000.	5000

Table 3
Term value cutoff needed to insure convergence of vibrational partition sums for methane isotopologues.

Maximum temperature (K) of converged Q_{vib}	Maximum term value in cm^{-1}	Number of term values for ($^{12}CH_4$, $^{12}CH_4$), ($^{12}CH_3D$, $^{13}CH_3D$)	
200	7000.	148	323
296	7000.	148	323
500	7000.	148	323
750	8000.	259	599
1000	10,000.	827	1888
1250	15,000.	7584	18,382
1500	18,000.	22,775	53,378
2000	22,000.	76,872	139,137
2500	27,500.	201,671	234,719

values, E_v, for each isotopologue of each molecule of this study are needed. These E_v files have been prepared and are available with the FORTRAN code discussed in section 4. The number of vibrational states in each file is given in Table 1; listed are the molecular isotopologue, the maximum rotational *term value*, the Q_r convergence (RC), the maximum vibrational *term value*, the Q_v convergence (VC), the number of vibrational *term values*, and the maximum temperature for which Q_v Q_r has converged. The convergence of the partition sums (Q_r and Q_v) is determined by the percent difference between Q determined by summing over all the *term values* and Q determined by summing over three-fourths of the *term values*. For some molecular isotopologues the number of *term values* is quite large. Users may want to truncate the list of E_v values; however, the convergence of the vibrational partition sum is dependent on temperature. Table 2 presents a rough guide relating the maximum term value to the maximum temperature for which Q_v is converged. Table 3 gives similar information as Table 2 for methane (see discussion in section 4). These cutoffs are discussed below when appropriate for each molecule/isotopologue combination.

3.1. H_2O

Nine isotopologues of water vapor were considered in this work: $H_2{}^{16}O$, $H_2{}^{18}O$, $H_2{}^{17}O$, $HD^{16}O$, $HD^{18}O$, $HD^{17}O$, $D_2{}^{16}O$, $D_2{}^{18}O$, and $D_2{}^{17}O$. The initial sets of *term values* are from Barber et al. (2006) and Tennyson et al. (2013) for $H_2{}^{16}O$, from Tennyson et al. (2009) for $H_2{}^{18}O$ and $H_2{}^{17}O$, from Tennyson et al. (2010) and Voronin et al. (2010) for $HD^{16}O$, from Tennyson et al. (2010) for $HD^{18}O$ and $HD^{17}O$, and from Simkó et al. (2017) and Tennyson et al. (2014) for $D_2{}^{16}O$, $D_2{}^{18}O$, and $D_2{}^{17}O$. These *term values* were taken and the rotational states of the ground vibrational state were extracted and the vibrational states with $J = 0$ states, designated E_v (note that these are called $G(\nu_1, \nu_2, \nu_3)$ in Herzberg's notation (Herzberg, 1960)), were extracted. It was observed that the rotational term values were not available for all states. This is due to the *first-principles* data not having complete attribution of the quantum numbers. To remedy this situation, the missing *term values* for the ground vibrational state were added using the smooth variation and pairing rules of Ma et al. (2011) for $H_2{}^{16}O$ and $HD^{16}O$. The rules show the energies of certain states labeled by the pseudo-quantum numbers

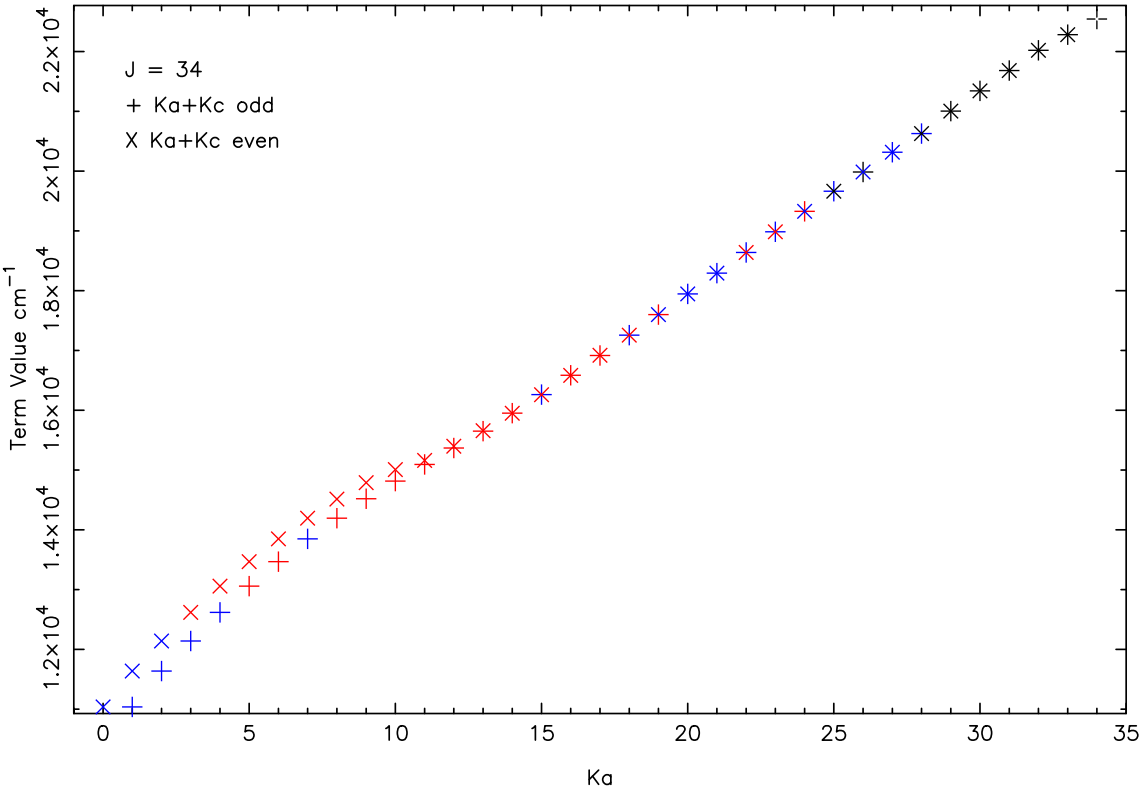

Fig. 1. The *term values* for $J = 34$ in the ground vibrational state of $H_2{}^{16}O$ versus K_a. The $K_a + K_c$ odd states are given by the + symbol and the $K_a + K_c$ even states are given by the × symbol. The MARVEL *term values* are given by blue symbols, the BT2 *term values* are given by red symbols, and the *term values* obtained using the rules of Ma et al. are given by black symbols. (For interpretation of the references to colour in this figure legend, the reader is referred to the web version of this article.)

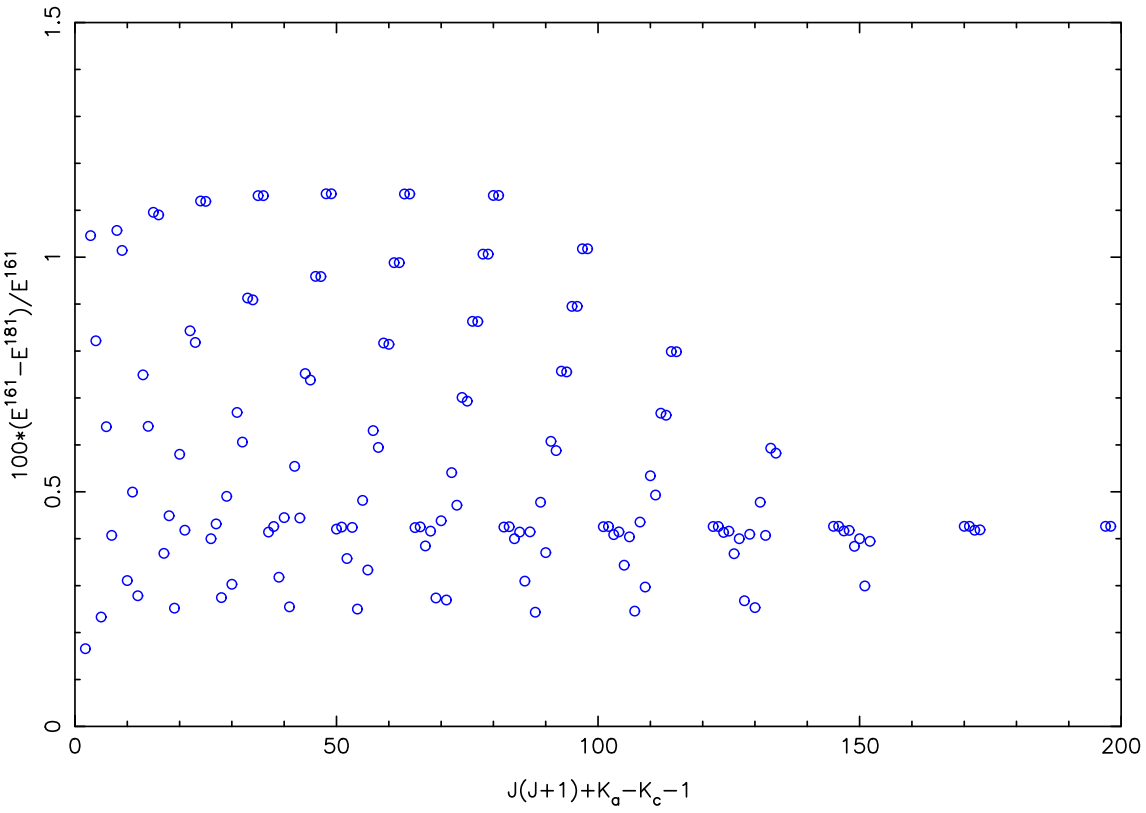

Fig. 2. The percent difference between the $H_2{}^{16}O$ and $H_2{}^{18}O$ *term values* versus an energy ordered index, $J(J+1) + K_a$-$K_c + 1$.

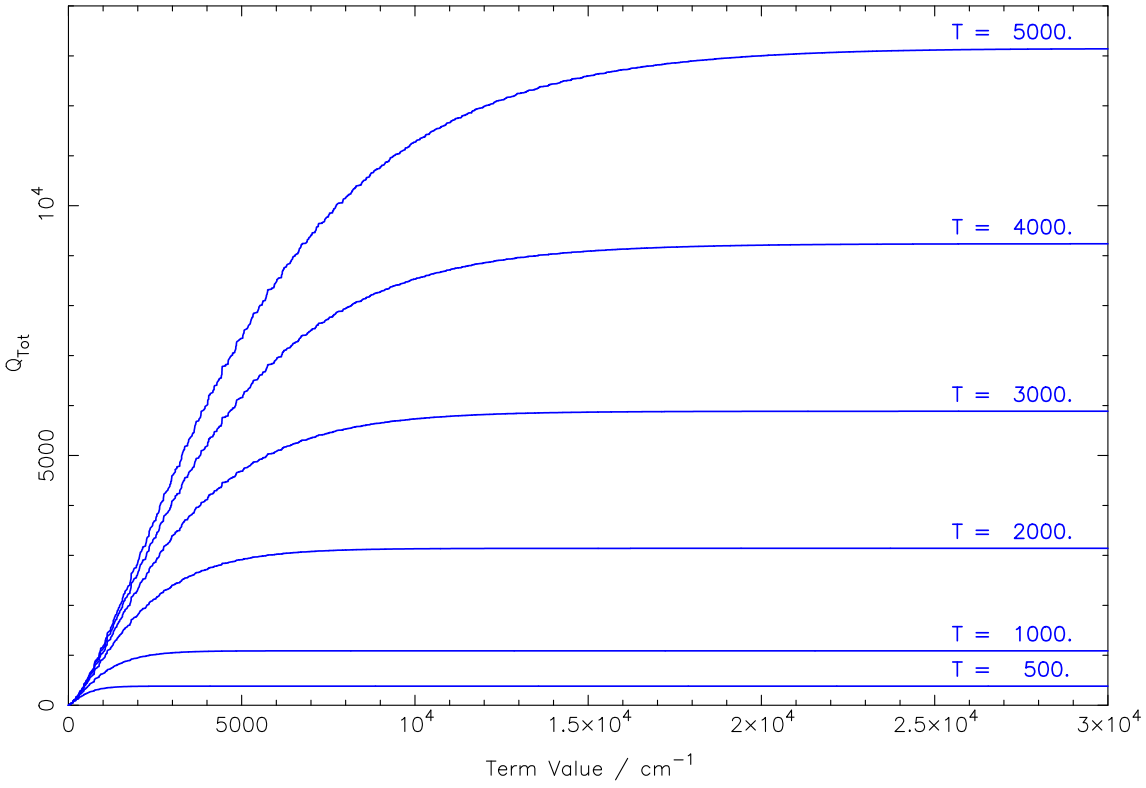

Fig. 3. The rotational internal partition sums for $H_2{}^{16}O$ versus *term value* for the following six temperatures: 500, 1000, 2000, 3000, 4000, and 5000 K.

K_a, K_c, which correspond to the projection of J along the inertia a and c axis, respectively, are equal or nearly equal. Fig. 1 shows the *term values* for $J = 34$ in the ground vibrational state of $H_2{}^{16}O$ versus K_a. In the figure the $K_a + K_c$ odd states are given by the + symbol and the $K_a + K_c$ even states are given by the × symbol. The MARVEL (Tennyson et al., 2013) *term values* are given by blue symbols, the BT2 (Barber et al., 2006) *term values* are given by red symbols, and the *term values* obtained using the rules of Ma et al. are given by black symbols. For the lesser abundant non-deuterated and singly deuterated isotopologues, $H_2{}^{18}O$, $H_2{}^{17}O$, $HD^{18}O$, and $HD^{17}O$, there are not enough MARVEL or labeled ab initio *term values* to apply the rules of Ma et al. The *term value* differences between the lesser abundant species and $H_2{}^{16}O$ or $HD^{16}O$ were considered. Fig. 2 shows the percent difference between the $H_2{}^{16}O$ and $H_2{}^{18}O$ *term values* versus an energy ordered index, $J(J+1) + K_a$-$K_c + 1$. The singly deuterated isotopologues show similar features. Since there is not a great difference in *term values*, when *term values* were missing in the files for $H_2{}^{18}O$, $H_2{}^{17}O$, $HD^{18}O$, and $HD^{17}O$ they were added using the $H_2{}^{16}O$ or $HD^{16}O$ data. This procedure allows the rotational partition sums to be converged to 5000 K and 4000 K for the H_2O and HDO isotopologues, respectively. The convergence of Q_r for $H_2{}^{16}O$ is shown in Fig. 3. Shown are the rotational internal partition sums versus *term value* for the following six temperatures: 500, 1000, 2000, 3000, 4000, and 5000 K. At 5000 K, Q_r is converged to better than 0.4%. Note that for the doubly deuterated isotopologues, the available *terms values* allow convergence of Q_r to 2000 K for $D_2{}^{16}O$, $D_2{}^{18}O$, and $D_2{}^{17}O$ (see Table 1).

The *term values* in the E_v files go to values large enough to ensure convergence of Q_v to 5000 K so the temperatures in Table 1 reflect the temperature for which Q_r converges.

Using the rotational *term values* and vibrational energies discussed above, the rotational and vibrational internal partition sums were computed for each isotopologue of water vapor in this study by direct summation. The calculations ranged from 1 to T_{max} in 1 K steps. Note, the Q_v determined is the LTE value and was used to check the NLTE calculations.

3.2. CO_2

The 12 isotopologues of CO_2 considered here are shown in Table 1. The vibrational states of CO_2 are labeled by $\nu_1\nu_2\ell_2\nu_3 n$, where ν_1, ν_2, ν_3 express the number of quanta activated for each normal mode; ℓ_2 is the ℓ value for the degenerate ν_2 normal mode and its overtones; the fifth integer is the nth component of the Fermi interacting ν_1 and $2\nu_2$ vibrational states, including their overtone and combination states (Rothman and Young, 1981; Toth et al., 2008). The vibrational energies in cm^{-1}, $E_v(\nu_1\nu_2\ell_2\nu_3 n)$, are from the *first-principles* calculations of Huang et al. (Huang et al., 2013; Huang et al., 2014). Because in the work of Huang et al. the rotational states were only calculated up to $J = 150$, the rotational *term values* were recalculated here for the ground vibrational state of each isotopologue up to $J = 226$ using the constants of (Majcherova et al., 2005) with updates from the Tomsk coauthors. The maximum values of the rotational *term values*, F_r, of the ground vibrational states and the vibrational energies for each isotopologue and the number of vibrational states are provided in Table 1. However, care must be taken as the partition sums are to be determined for Q_v and Q_r separately and the product approximation used for the NLTE total internal partition sum. The four isotopologues of carbon dioxide, $^{12}C^{16}O_2$, $^{13}C^{16}O_2$, $^{12}C^{18}O_2$, $^{13}C^{18}O_2$, have equivalent oxygen atoms with zero spin nuclei (i.e. Bose particles). For these isotopologues, vibrational states with $\ell_2 = 0$ only even J levels are allowed when ν_3 is even and only odd J levels exist when ν_3 is odd, however, when $\ell_2 > 0$ all J levels exist. The total internal partition sum can be written as

$$Q(T) = \sum_{\text{all states}} g\,e^{-E_{vr}/kT} = g\,e^{-E(00001,J)/kT} + g\,e^{-E(01101,J)/kT} + g\,e^{-E(10001,J)/kT} + g\,e^{-E(00011,J)/kT} + g\,e^{-E(10002,J)/kT} + g\,e^{-E(11101,J)/kT} + g\,e^{-E(01111,J)/kT} + g\,e^{-E(02201,J)/kT} + \cdots \tag{26}$$

This expression can be rewritten by collecting terms with $\ell_2 = 0$ and with $\ell_2 > 0$

$$\begin{aligned} Q(T) &= \left\{ g e^{-E(00001,J)/kT} + g e^{-E(10001,J)/kT} + g e^{-E(00011,J)/kT} + g e^{-E(10002,J)/kT} + \cdots \right\} \\ &+ \left\{ g e^{-E(01101,J)/kT} + g e^{-E(11101,J)/kT} + g e^{-E(01111,J)/kT} + g e^{-E(02201,J)/kT} + \cdots \right\} \\ &= \sum_{\substack{\text{all states} \\ \text{with}\,\ell_2=0}} g e^{-E(v,J)/kT} + \sum_{\substack{\text{all states} \\ \text{with}\,\ell_2>0}} g e^{-E(v,J)/kT} \end{aligned} \tag{27}$$

Taking the ro-vibrational energy as a sum of the vibrational and rotational parts, $E_{vr} = E_v + E_r$ and realizing that when $\ell_2 = 0$ only even J levels are allowed when ν_3 is even and only odd J levels exist when ν_3 is odd and when $\ell_2 > 0$ all J levels, $J \geqq \ell_2$, are allowed, gives

$$\begin{aligned} Q(T) = &\left(\sum_{\substack{\text{all vib states} \\ \text{with}\,\ell_2=0,\nu_3\,\text{even}}} g e^{-E_v/kT} \right) \left(\sum_{\substack{J=0 \\ \text{even only}}}^{J_{max}} g_J e^{-E_r/kT} \right) + \left(\sum_{\substack{\text{all vib states} \\ \text{with}\,\ell_2=0,\nu_3\,\text{odd}}} g e^{-E_v/kT} \right) \left(\sum_{\substack{J=\ell_2 \\ \text{odd only}}}^{J_{max}} g_J e^{-E_r/kT} \right) + \\ &\left(\sum_{\substack{\text{all vib states} \\ \text{with}\,\ell_2>0}} g e^{-E_v/kT} \right) \left(\sum_{\substack{J=\ell_2 \\ \text{even\&odd}}}^{J_{max}} g_J e^{-E_r/kT} \right) \end{aligned} \tag{28}$$

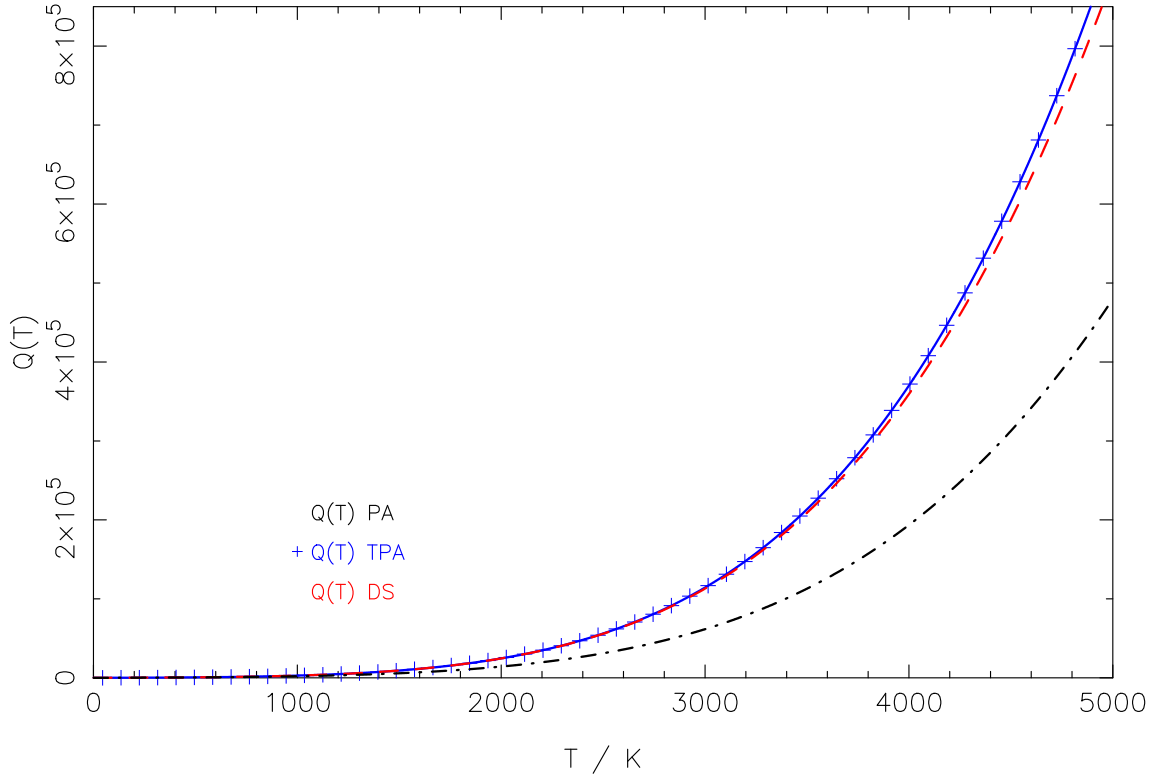

Fig. 4. The comparison of the TPA and the PA to the TIPS determined by direct sum. Shown are the TIPS determined by direct summation (red dashed line), the TIPS determeined via the TPA (blue solid line with + symbols), and the TIPS determined via the PA (black dot-dashed line) versus temperature. (For interpretation of the references to colour in this figure legend, the reader is referred to the web version of this article.)

or

$$Q(T) = \sum_{\ell_2=0}^{\nu_3\,\text{even}} Q_v(T) \times Q_r(J\,\text{even}) + \sum_{\ell_2=0}^{\nu_3\,\text{odd}} Q_v(T) \times Q_r(J\,\text{odd}) + Q_v^{\ell_2>0}(T) \times Q_r(all\ J) \quad (29)$$

This expression is labeled the triple product approximation (TPA). Eq. (29) must be used for the symmetric Boze system CO_2 isotopologues rather than the product approximation, Eq. (8). In order to make these calculations, the rotational *terms values* for the (01101) vibrational state were extracted from the work of Huang et al., fit to determine the rotational constants, and calculations were made up to $J = 226$. Note, for the rotational *terms values* for (01101), the vibrational energy, E_v(01101), must be subtracted from the energies reported by Huang et al. (see Eq. (29)). The comparison of the TPA and the PA to the TIPS determined from a direct sum in the work of Gamache et al. (2017) is presented in Fig. 4. Shown are the TIPS determined by direct summation (red dashed line), the TIPS determeined via the TPA (blue solid line with + symbols), and the TIPS determined via the PA (black dot-dashed line) versus temperature. The PA TIPS is in error by 4% at 296 K, 29% at 1000 K, and 46% at 5000 K.

Using the *term values* and vibrational energies discussed above, the rotational and vibrational internal partition sums were computed for each isotopologue of carbon dioxide in this study by direct summation. While the vibrational partition sums are converged to 4000 K, the rotational partition sums are only converged to 3000 K, so T_{max} was set to 3000 K (see Table 1). The calculations ranged from 1 to 3000 K in 1 K steps. Note, the Q_v determined is the LTE value and was used to check the NLTE calculations.

3.3. O_3

The vibrational and rotational constants used in this work are from the "Ozone Spectroscopy and Molecular Properties" (S&MPO) databank (Babikov et al., 2014) updated in 2020. For rare isotopic species these data were obtained from the analyses of experimental spectra recorded in the Groupe de Spectrométrie Moléculaire et Atmosphérique (GMSA, Université de Reims) with the help of *first-principles* predictions carried out in Tomsk State University, Russia. The vibrational fundamentals, ν_1, ν_2, and ν_3 were used to generate vibrational energies, $E_v(\nu_1, \nu_2, \nu_3)$, with up to 9 quanta within the harmonic approximation of (Herzberg, 1960). The rotational partition sums used the analytical formula of (Watson, 1988). Calculations of Q_v and Q_r were made from 1 to 1000 K in 1 K steps.

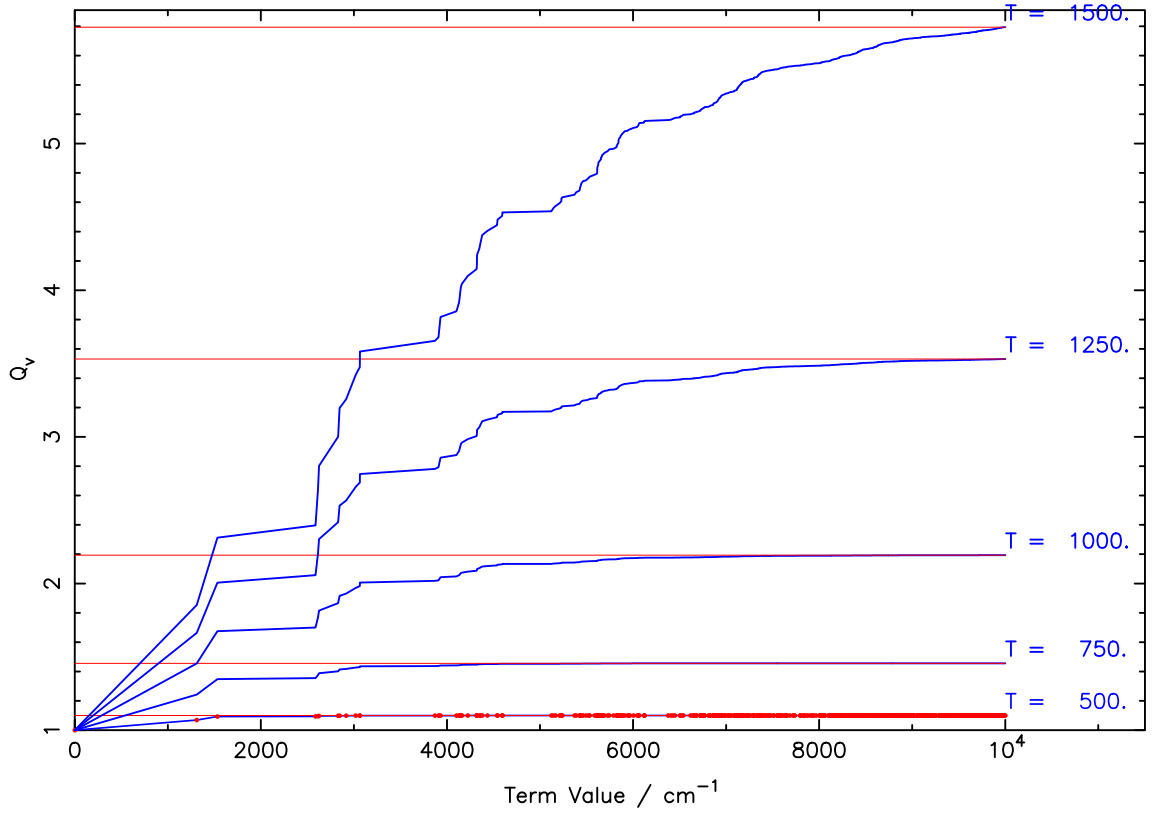

Fig. 5. The calculation of Q_v for $^{12}CH_4$ as a function of the vibrational energy for a summation up to 10,000 cm^{-1}. Shown are Q_v values (blue lines) for the temperatures of 500, 750, 1000, 1250, and 1500 K versus the vibrational energy in cm^{-1}. The red line indicates the final Q_v value after summing over all the energies and hence gives an indication of convergence. Also shown on the 500 K curve are the values of the vibrational energies (red dots) showing the polyad structure and the density of states. (For interpretation of the references to colour in this figure legend, the reader is referred to the web version of this article.)

3.4. N_2O

The vibrational fundamentals and rotational constants of Toth (1986) were used for the five isotopologues of nitrous oxide of this study: $^{14}N_2{}^{16}O$, $^{14}N^{15}N^{16}O$, $^{15}N^{14}N^{16}O$, $^{14}N_2{}^{18}O$, and $^{14}N_2{}^{17}O$. The $E_v(\nu_1, \nu_2, \ell_2, \nu_3)$ values were generated using Eq. (II-284) of Herzberg (1960) and E_v data from HITRAN2020 (Gordon et al., 2021) to determine the constants. The $E_v(\nu_1, \nu_2, \ell_2, \nu_3)$ data were then computed with up to 9 quanta of each fundamental frequency. The Q_r data were generated using the McDowell formula for linear molecules (McDowell, 1988). Calculations were made from 1 to 5000 K in 1 K steps and are converged at all temperatures.

3.5. CO

Nine isotopologues of CO are studied here: $^{12}C^{16}O$, $^{13}C^{16}O$, $^{12}C^{18}O$, $^{12}C^{17}O$, $^{13}C^{18}O$, $^{13}C^{17}O$, $^{14}C^{16}O$, $^{14}C^{18}O$, and $^{14}C^{17}O$. The rotational *term values* ($v = 0$) and the E_v values ($J = 0$) were extracted from the work of Li et al. (2015). The calculations were made for each isotopologue in the electronic ground state with $v \leq 41$ and $J \leq 150$. For all isotopologues, the E_v values are complete to 63,802 cm^{-1} or greater and the *rotational term values* (on the ground vibrational state) are complete to 35,138 cm^{-}1 or greater. Q_v and Q_r were computed at temperatures from 1 to 5000 K, in 1 K steps using the E_v values and *term values* discussed above and the resulting partition sums are converged at all temperatures for each isotopologue.

3.6. CH_4

Four isotopologues were considered in this work: $^{12}CH_4$, $^{13}CH_4$, $^{12}CH_3D$, and $^{13}CH_3D$. For the principal isotopologue, an effective Hamiltonian calculation of the ground vibrational state *term values* was done up to $J = 80$, giving values complete to 30,424 cm^{-1} ensuring convergence at all temperatures. For $^{13}CH_4$, the rotational constants are from Dang-Nhu et al. (1979) and were used to compute Q_r values using McDowell's spherical-top formula (McDowell, 1987). The rotational constants for $^{12}CH_3D$ are from Tarrago et al. (1987), and those for $^{13}CH_3D$ are from Ulenikov et al. (2000), and were used to compute Q_r values using McDowell's symmetric top formula (McDowell, 1990).

Calculations were made for the E_v values ($J = 0$) for $^{12}CH_4$, $^{13}CH_4$, $^{12}CH_3D$ and $^{13}CH_3D$. For semirigid molecules without large amplitude vibrations, like methane and its isotopologues, the normal mode representation turns out to be an excellent choice because it provides an adequate description of the nuclear motions. In this context, the normal mode kinetic energy operator was built in the frame of the Eckart-Watson (EW) formalism (Watson, 1968). The curvilinear potential energy surface (PES) reported by Nikitin et al. (2011) was transformed and Taylor-expanded in mass-dependent normal mode coordinates q adapted to the T_d and C_{3v} point groups. Both the kinetic and potential parts have been expanded at order 14 in q and reduced at order 7 using the technique described in Rey et al. (2018). For a full account of symmetry, the use of the irreducible tensor operator technique was used to build the EW Hamiltonian and ro-vibrational basis functions following Rey et al. (Rey et al., 2012; Rey et al., 2014) while energy levels were computed by a variational method.

The $J = 0$ vibrational problem was first solved using a direct product of harmonic oscillator functions where a "pruned" vibrational basis was considered by selecting a limited number of functions through the criterion

$$F(n) = \sum_{i=1}^{M} k_i v_i \leq n \tag{29}$$

with $M = 4$ for T_d species and $M = 6$ for C_{3V} species. Here, $v_i = 0, \ldots, n$ and k_i are weighting coefficients. For this work, $n = 15$ and $k_i = \{1;1;1.1;1\}$ for $^{12}CH_4$ and $^{13}CH_4$ and $n = 14$ and $k_i = \{1.2;1.1;1;1.2,1,1\}$ for $^{12}CH_3D$ and $^{13}CH_3D$, resulting in 36,889, 32,903, 69,751, 101,912 and 105,888 functions for the symmetry blocks $\{A_1, A_2, E, F_1, F_2\}$ and 70,552, 65,855 and 136,374 functions for the symmetry blocks $\{A_1, A_2, E\}$, respectively. In contrast to the effective polyad models, variational calculations require the diagonalization of very large matrices for $J > 0$, even for computing *pure* rotational energy levels. To this end, a set of vibrational reduced eigenfunctions obtained from the projection technique (Rey et al., 2018) was introduced to drastically reduce dimensionality of the full problem, making thus calculations feasible even for high J values. These vibrational energies were used to compute the Q_v values and were also put into files to compute $\widetilde{Q}_v$ from the code of section 4.

The number of vibrational levels for all isotopologues of methane considered here is large. Because of the density of states and the polyad structure of the vibrational levels, Table 2 should not be used to determine the convergence of Q_v. Convergence plots were made for temperatures from 200 to 2500 K. Fig. 5 shows the calculation of Q_v as a function of the vibrational energy for a summation up to 10,000 cm^{-1}. Shown are Q_v values (blue lines) for the temperatures of 500, 750, 1000, 1250, and 1500 K versus the vibrational energy in cm^{-1}. The red line indicates the final Q_v value after summing over all the energies and hence gives an indication of convergence. Also shown on the 500 K curve are the values of the vibrational energies (red dots) showing the polyad structure and the density of states. Looking at the curves, it is clear that summing energies up to 10,000 cm^{-1} gives Q_vs that are only converged up to 1000 K. The erratic structure in the curves at low energy and for higher temperatures is due to the polyad structure and the density of states. Table 3 should be used to determine the convergence of Q_v for the methane isotopologues.

The Q_v and Q_r values were computed from 1 to 2500 k in 1 K steps.

3.7. NO

Nitric oxide is an open shell molecule with a $^2\Pi_{1/2}$ ground electronic state and a close lying $^2\Pi_{3/2}$ electronic state, roughly 120 cm^{-1} above the $^2\Pi_{1/2}$ electronic state. There is lambda doubling that gives rise to e and f energy states. The states are labeled by J and $F = J \pm 1{,}0$ and e or f. The total internal partition sum can be written as

$$Q(T) = \sum_{\text{all states } i} g_i \, e^{-hcE_i/kT} = \sum_{\substack{\text{all}^2\Pi_{1/2} \\ \text{states } a}} g_a \, e^{-hcE_a/kT} + \sum_{\substack{\text{all}^2\Pi_{3/2} \\ \text{states } b}} g_b \, e^{-hcE_b/kT} \tag{30}$$

Assuming that the vibrational levels are the same for the $^2\Pi_{1/2}$ and $^2\Pi_{3/2}$ electronic states, as shown by Amiot et al. (1978), the energy can be written as $E_a\left(^2\Pi_{1/2}\right) = E_v + E_r\left(^2\Pi_{1/2}\right)$ and $E_b\left(^2\Pi_{3/2}\right) = E_v + E_r\left(^2\Pi_{3/2}\right)$. Eq. (30) can be rewritten as a product approximation.

$$Q(T) = \sum_{\substack{\text{all} \\ \text{vibrational} \\ \text{states}}} g_v \, e^{-hcE_v/kT} \times \sum_{\substack{\text{all}^2\Pi_{1/2} \\ \text{rotational} \\ \text{states}}} g_r \, e^{-hcE_r/kT} + \sum_{\substack{\text{all} \\ \text{vibrational} \\ \text{states}}} g_v \, e^{-hcE_v/kT} \times \sum_{\substack{\text{all}^2\Pi_{3/2} \\ \text{rotational} \\ \text{states}}} g_r \, e^{-hcE_r/kT} \tag{31}$$

Because the vibrational states are the same, the product approximation becomes

$$Q(T) = \sum_{\substack{\text{all} \\ \text{vibrational} \\ \text{states}}} g_v \, e^{-hcE_v/kT} \times \left(\sum_{\substack{\text{all}^2\Pi_{1/2} \\ \text{rotational} \\ \text{states}}} g_r \, e^{-hcE_r/kT} + \sum_{\substack{\text{all}^2\Pi_{3/2} \\ \text{rotational} \\ \text{states}}} g_r \, e^{-hcE_r/kT} \right) \tag{32}$$

which is of the form of Eq. (8).

For the $^{14}N^{16}O$, $^{15}N^{16}O$, and $^{14}N^{18}O$ isotopologues of nitric oxide, the rotational *term values* were calculated for the $^2\prod_{1/2e}$, $^2\prod_{1/2f}$, $^2\prod_{3/2e}$, and $^2\prod_{3/2f}$, states using the molecular constants of Amiot et al. (1978) up to $J = 149.5$, $F = 150.5$ and are complete to 35,391, 34,233, and 33,693 cm^{-1}, respectively. These *term values* were used to compute Q_r by direct sum.

The fundamental frequency for each isotopologue, ω_i, were taken from Amiot et al. (1978) and Meerts (1976) were used to determine Q_v via the HA and to generated the E_v files. However, Aimot et al. report a value for v = 2 for $^{14}N^{16}O$, which replaced the HA value in the E_v file. Both partition sums, Q_v and Q_r, were computed from 1 to 5000 k in 1 K steps for each isotopologue.

3.8. NO_2

Calculations of Q_v and Q_r were made for the $^{14}N^{16}O_2$ and $^{15}N^{16}O_2$ isotopologues of nitrogen dioxide. The rotational and vibrational constants were taken from Perrin et al. (1988) for $^{14}N^{16}O_2$ and from Perrin et al. (2015) for $^{15}N^{16}O_2$. The analytical formula of Watson (1988) was used to determine Q_r. Note, the state independent statistical factor is determined by considering that both isotopologues are Bose particles, so half of the states are missing. However, lambda doubling adds a factor of 2. These factors must be multiplied by the nuclear spin factor of the N atom giving: ½ ·2·(2·1 + 1) = 3 for $^{14}N^{16}O_2$ and ½ ·2·(2·½ + 1) = 2 for $^{15}N^{16}O_2$. The vibrational fundamentals, ν_1, ν_2, and ν_3 were used to generate vibrational energies, $E_v(\nu_1, \nu_2, \nu_3)$, with up to 9 quanta within the harmonic approximation of Herzberg (1960). The final partition functions were calculated from 1 to 5000 K in 1 K steps.

3.9. OH

Three isotopologues of the hydroxyl radical were considered in this work: ^{16}OH, ^{18}OH, and ^{16}OD. The *rotational term values* of the principal isotopologue were taken from Brooke et al. (2016) and are complete to $J = 58.5$, $E = 46{,}065.460\ 3$ cm^{-1}. For the ^{18}OH and ^{16}OD isotopologues, the rotational term values for the $^2\prod_{1/2}$, $^2\prod_{3/2}$, and $^2\Sigma_{1/2}$, states were calculated using the formalism of Beaudet and Poynter (1978), which includes the fine structure interaction and lambda doubling. This procedure generated energies complete to 42,000 cm^{-1} for ^{18}OH, and 39,000 cm^{-1} for ^{16}OD. The rotational partition sums were calculated by direct summation over the *rotational term values*. The vibrational fundamentals were taken from Beaudet and Poynter (1978) and used to generate harmonic approximation vibrational energies, E_v, with up to $v = 13$ giving maximum energies of 33,086, 31,586, 32,643, for ^{16}OH,

^{18}OH, and ^{16}OD, respectively. The final partition functions were calculated from 1 to 5000 K in 1 K steps.

4. Recall of the NLTE partition sums

Eqs. (24) and (25) show that to correctly determine the intensity of a spectral line in NLTE conditions both $Q_r(T)$ and $\widetilde{Q}_v(T)$ are needed. The $Q_r(T)$ values can easily be precalculated as a function of temperature, stored in the code for fast recall. Computing $\widetilde{Q}_v(T)$ is more difficult in that a file of vibrational temperatures is needed for each layer of the atmosphere. To accomplish this task, a FORTRAN code was written to store $Q_r(T)$ and $Q_v(T)$ data and recall the values as a function of temperature using Lagrange interpolation and using files of vibrational wavenumbers and temperatures to calculate $\widetilde{Q}_v(T)$for the atmospheric layer in question. The code, NLTE_TIPS_2021.FOR, stores $Q_r(T)$ and $Q_v(T)$ from 1 to 20 K in 1 K steps and then the values at every 10 K to the maximum temperature of the computations for a given molecule. The user is prompted for the molecule, isotopologue, and kinetic temperature to determine $Q_r(T)$ and $Q_v(T)$. The code uses a 4-point Lagrange interpolation scheme, similar to earlier versions of TIPS (Fischer et al., 2003; Laraia et al., 2011). The value of $Q_v(T)$ is only computed for reference, it is not used in Eqs. (24) or (25). The computation for $\widetilde{Q}_v(T)$ is made by summing over the vibrational energies with the appropriate T_ν values for the atmospheric layer in question. There are files for each isotopologue of this study provided with the code. These T_ν files are named by molecule_isotopologue#_layer.dat; for example, for $^{16}O^{12}C^{18}O$ the file is CO2_3_002.dat for layer 2 of the atmosphere, that for the first layer for $^{16}O^{14}N^{16}O$ is NO2_1_001.dat. The file structure is vibrational state in HITRAN notation, the degeneracy of the state, the vibrational energy in cm^{-1}, and the vibrational temperature of the state with (A15,F7.1,F15.4,F7.1) format. A value of −1.0 for the vibrational temperature implies $T_\nu = T_{\text{kinetic}}$. Users must solve the statistical equilibrium equations for each layer of the atmosphere they are studying and then enter the resulting T_ν values into the appropriate layer file. The work of López-Puertas et al. (1986b) Figs. 2, 7, and 11 show the vibrational temperatures of particular CO_2 isotopologue vibrational bands as a function of altitude. The code currently can consider 999 atmospheric layers. The code uses the MIT license (see code for details).

A note about the T_ν files, most of the calculations have a $T_{\max}$ equal to 5000 K. To ensure convergence of $\widetilde{Q}_v(T)$, the vibrational states were determined to high energies. For applications at lower temperatures the files can be truncated appropriately. Table 2 provides a guide to the cutoff in energy as a function of the $\widetilde{Q}_v(T)$ for H_2O, CO_2, O_3, N_2O, CO, NO, NO_2, and OH and Table 3 provides the cutoff in energy as a function of the $\widetilde{Q}_v(T)$ for CH_4. Users should use caution when truncating the files.

5. Conclusions

The general theory of applying radiative transfer to conditions where non-local thermodynamics equilibrium (NLTE) must be considered is presented and the calculation of the NLTE partition sums is outlined. Rotational and vibrational partition sums were made for nine molecules, forty-five isotopologues, of importance in planetary atmospheres: H_2O, CO_2, O_3, N_2O, CO, CH_4, NO, NO_2, and OH. The calculations are made at temperatures from 1 K to $T_{\max}$, where the maximum temperatures are determined for each isotopologue such that Q_v and Q_r are converged, see Table 1 for details. These data are presented in Table 1. The calculations of Q_v and Q_r are described for each molecule/isotopologue combination. A FORTRAN code, NLTE_TIPS_2021.for, to compute the NLTE $\widetilde{Q}_v(T)$, the recall of Q_r, and the needed vibrational energy files are provided. Truncating the list of vibrational energies is possible for some lower temperature applications. To aid users, tables of the maximum vibrational energies needed for convergence of $\widetilde{Q}_v(T)$as a function of temperature are presented for the molecules in general (Table 2) and separately for methane (Table 3). The code uses the MIT license and it and the needed vibrational energy files and can be downloaded at http://faculty.uml.edu/Robert_Gamache, at www.HITRAN.org, or from zenodo.org (https://doi.org/10.5281/zenodo.6108004).

Declaration of Competing Interest

None.

Acknowledgements

B. Vispoel is pleased to acknowledge le Fonds de la Recherche Scientifique – FNRS for post-doctoral financial support. The GSMA Reims group acknowledges the support from CNRS (France) in the frame of the International Research Project SAMIA with IAO-Tomsk. M.R., V.T. and A.N. acknowledge the support from French-Russian ANR-RNF TEMMEX project (grants ANR-21-30CE-0053-01 and RNF 22-42-09022). JT and SY thank ERC's Advanced Investigator Awards 267219 (2011-16) and 883830 225 (2020-25), as well as STFC as part of the UCL consolidated grant ST/R000476/1. The work in Tomsk was supported by Ministry of Science and Higher Education of the Russian Federation. The work in Budapest was supported by NKFIH under grant no. K138233.

References

Amiot, C., Bacis, R., Guelachvili, G., 1978. Infrared study of the X2Π $\nu = 0, 1, 2$ levels of $^{14}N^{16}O$. Preliminary results on the $\nu = 0, 1$ levels of $^{14}N^{17}O$, $^{14}N^{18}O$, and $^{15}N^{16}O$. Can. J. Phys. 56, 251–265.

Babikov, Y.L., Mikhailenko, S.N., Barbe, A., Tyuterev, V.G., 2014. S&MPO – an information system for ozone spectroscopy on the WEB. J. Quant. Spectrosc. Radiat. Transf. 145, 169–196 (updated at http://smpo.univ-reims.fr and https://smpo.tsu.ru/).

Barber, R.J., Tennyson, J., Harris, G.J., Tolchenov, R.N., 2006. A high-accuracy computed water line list. Mon. Not. R. Astron. Soc. 368, 1087–1094.

Beaudet, R.A., Poynter, R.L., 1978. Mirowave spectra of molecules of astrophysical interest. XII. Hydroxyl radical. J. Phys. Chem. Ref. Data 7, 311–313.

Bernath, P.F., 2014. Molecular opacities for exoplanets. Phil. Trans. R. Soc. A 372, 20130087.

Brooke, J.S.A., et al., 2016. Line strengths of rovibrational and rotational transitions in the ground state of OH. J. Quant. Spectrosc. Radiat. Transf. 168, 142–157.

Dang-Nhu, M., Pine, A.S., Robiette, A.G., 1979. Spectral intensities in the ν_3 bands of $^{12}CH_4$ and $^{13}CH_4$. J. Mol. Spectrosc. 77, 57–68.

Däppen, W., Mihalas, D., Hummer, D.G., Mihalas, B.W., 1988. The equation of state for stellar envelopes III. Thermodynamic quantities. Astron. J. 332, 261–270.

Delahaye, T., et al., 2021. The 2020 edition of the GEISA spectroscopic database. J. Mol. Spectrosc. 380, 111510.

Dudás, E., et al., 2020. High-temperature hypersonic Laval nozzle for non-LTE cavity ringdown spectroscopy. J. Chem. Phys. 152, 134201.

Edwards, D.P., Lopez-Puertas, M., Lopez-Valverde, M.A., 1993. Non-local thermodynamic equilibrium studies of the 15-μm bands of CO_2 for atmospheric remote sensing. J. Geophys. Res. 98, 14955.

Edwards, D.P., López-Puertas, M., Gamache, R.R., 1998a. The non-LTE correction to the vibrational component of the internal partition sum for atmospheric calculations. J. Quant. Spectrosc. Radiat. Transf. 59, 423–436.

Edwards, D.P., López-Puertas, M., Gamache, R.R., 1998b. The non-LTE correction to the vibrational component of the internal partition sum for atmospheric calculations. J. Quant. Spectrosc. Radiat. Transf. 59, 423–436.

Fischer, J., Gamache, R.R., Goldman, A., Rothman, L.S., Perrin, A., 2003. Total internal partition sums for molecular species on the 2000 edition of the HITRAN database. J. Quant. Spectrosc. Radiat. Transf. 82, 401–412.

Fossati, L., et al., 2020. A data-driven approach to constraining the atmospheric temperature structure of the ultra-hot Jupiter KELT-9b. A&A. 643.

Gamache, R.R., Rothman, L.S., 1992. Extension of the Hitran database to non-LTE applications. J. Quant. Spectrosc. Radiat. Transf. 48, 519–525.

Gamache, R.R., Hawkins, R.L., Rothman, L.S., 1990. Total internal partition sums in the temperature range 70-3000K: atmospheric linear molecules. J. Mol. Spectrosc. 142, 205–219.

Gamache, R.R., Kennedy, S., Hawkins, R., Rothman, L.S., 2000. Total internal partition sums for molecules in the terrestrial atmosphere. J. Mol. Struct. 517-518, 413–431.

Gamache, R.R., et al., 2017. Total internal partition sums for 166 isotopologues of 51 molecules important in planetary atmospheres: application to HITRAN2016 and beyond. J. Quant. Spectrosc. Radiat. Transf. 203, 70–87.

Gordon, I.E., et al., 2021. The HITRAN2020 molecular spectroscopic database. J. Quant. Spectrosc. Radiat. Transf. 110, 107949.

Herzberg, G., 1960. Molecular Spectra and Molecular Structure II. In: Infrared and Raman Spectra of Polyatomic Molecules. D. Van Nostrand Company, Inc., New Jersey.

Huang, X., Freedman, R.S., Tashkun, S.A., Schwenke, D.W., Lee, T.J., 2013. Semi-empirical $^{12}C^{16}O_2$ IR line lists for simulations up to 1500 K and 20,000 cm^{-1}. J. Quant. Spectrosc. Radiat. Transf. 130, 134–146.

Huang, X., Gamache, R.R., Freedman, R.S., Schwenke, D.W., Lee, T.J., 2014. Reliable InfraRed line lists for $^{13}CO_2$ Isotopologues up to E'=18,000 cm^{-1} and 1500K, with line shape parameters. J. Quant. Spectrosc. Radiat. Transf. 147, 134–144.

Hummer, D.G., Mihalas, D., 1988. The equation of state for stellar envelopes I. an occupation probability formalism for the truncation of internal partition functions. Astron. J. 331, 794–814.

Kutepov, A.A., Gusev, O.A., Ogibalov, V.P., 1998. Solution of the non-LTE problem for molecular gas in planetary atmospheres: superiority of accelerated lambda iteration. J. Quant. Spectrosc. Radiat. Transf. 60, 199–220.

Laraia, A.L., Gamache, R.R., Lamouroux, J., Gordon, I.E., Rothman, L.S., 2011. Total internal partition sums to support planetary remote sensing. Icarus. 215, 391–400.

Li, G., et al., 2015. Rovibrational line lists for nine isotopologues of the CO molecule in the $X^1\Sigma^+$ ground electronic state. Astrophys. J. Suppl. Ser. 216, 15.

López-Puertas, M., Rodrigo, R., López-Moreno, J.J., Taylor, F.W., 1986a. A non-LTE radiative transfer model for infrared bands in the middle atmosphere. II. CO_2 (2.7 and 4.3 μm) and water vapour (6.3 μm) bands and $N_2(1)$ and $O_2(1)$ vibrational levels. J. Atmosph. Terrestr. Phys. 48, 749–764.

López-Puertas, M., Rodrigo, R., Molina, A., Taylor, F.W., 1986b. A non-LTE radiative transfer model for infrared bands in the middle atmosphere. I. Theoretical basis and application to CO_2 15 μm bands. J. Atmosph. Terrestr. Phys. 48, 729–748.

López-Puertas, M., López-Valverde, M.A., Taylor, F.W., 1990. Studies of solar heating by CO_2 in the upper atmosphere using a non-LTE model and satellite data. J. Atmos. Sci. 47, 809–822.

Ma, Q., Tipping, R.H., Lavrentieva, N.N., 2011. Pair identity and smooth variation rules applicable for the spectroscopic parameters of H_2O transitions involving high-J states. Mol. Phys. 109, 1925–1941.

Majcherova, Z., et al., 2005. High-sensitivity CW-cavity ringdown spectroscopy of $^{12}CO_2$ near 1.5μm. J. Mol. Spectrosc. 230, 1–21.

McDowell, R.S., 1987. Rotational partition functions for spherical-top molecules. J. Quant. Spectrosc. Radiat. Transf. 38, 337–346.

McDowell, R.S., 1988. Rotational partition fuctions for linear molecules. J. Chem. Phys. 88, 356–361.

McDowell, R.S., 1990. Rotational partition functions for symmetric-top molecules. J. Chem. Phys. 93, 2801–2811.

Meerts, W.L., 1976. A theoretical reinvestigation of the rotational and hyperfine lambda doubling spectra of diatomic molecules with a 2Π state: the spectrum of no. Chem. Phys. 14, 421–425.

Mihalas, D., Däppen, W., Hummer, D.G., 1988. The equation of state for stellar envelopes II. Algorithm and selected results. Astron. J. 331, 815–825.

Mohr, P.J., Newell, D.B., Taylor, B.N., 2016. CODATA recommended values of the fundamental physical constants: 2014. Rev. Mod. Phys. 88, 035009.

Nikitin, A.V., Rey, M., Tyuterev, V.G., 2011. Rotational and vibrational energy levels of methane calculated from a new potential energy surface. Chem. Phys. Lett. 501, 179–186.

Perrin, A., Flaud, J.-M., Peyret, C., Carli, C., Carlotti, M., 1988. The far infrared spectrum of $^{14}N^{16}O_2$ Electron spin-rotation and hyperfine Fermi contact resonances in the ground state. Mol. Phys. 63, 791–810.

Perrin, A., Toon, G., Orphal, J., 2015. Detection of atmospheric $^{15}NO_2$ in the ν_3 spectral region (6.3 μm). J. Quant. Spectrosc. Radiat. Transf. 154, 91–97.

Rey, M., Nikitin, A.V., Tyuterev, V.G., 2012. Complete nuclear motion Hamiltonian in the irreducible normal mode tensor operator formalism for the methane molecule. J. Chem. Phys. 136, 244106.

Rey, M., Nikitin, A.V., Tyuterev, V.G., 2014. Accurate first-principles calculations for $^{12}CH_3D$ infrared spectra from isotopic and symmetry transformations. J. Chem. Phys. 141, 044316.

Rey, M., Chizhmakova, I.S., Nikitin, A.V., Tyuterev, V.G., 2018. Understanding global infrared opacity and hot bands of greenhouse molecules with low vibrational modes from first-principles calculations: the case of CF_4. Phys. Chem. Chem. Phys. 20, 21008–21033.

Rothman, L.S., Young, L.D.G., 1981. Infrared energy levels and intensities of carbon dioxide—II. J. Quant. Spectrosc. Radiat. Transf. 25, 505–524.

Simkó, I., et al., 2017. Recommended ideal-gas thermochemical functions for heavy water and its substituent Isotopologues. J. Phys. Chem. Ref. Data 46, 023104.

Swain, M.R., Vasisht, G., Tinetti, G., 2008. The presence of methane in the atmosphere of an extrasolar planet. Nature. 452, 329–331.

Tarrago, G., Delaveau, M., Fusina, L., Guelachvili, G., 1987. Absorption of $^{12}CH_3D$ at 6–10 μm: triad ν_3, ν_5, ν_6. J. Mol. Spectrosc. 126, 149–158.

Tennyson, J., et al., 2009. IUPAC critical evaluation of the rotational–vibrational spectra of water vapor. Part I—energy levels and transition wavenumbers for $H_2{}^{17}O$ and $H_2{}^{18}O$. J. Quant. Spectrosc. Radiat. Transf. 110, 573–596.

Tennyson, J., et al., 2010. IUPAC critical evaluation of the rotational–vibrational spectra of water vapor. Part II: energy levels and transition wavenumbers for $HD^{16}O$, $HD^{17}O$, and $HD^{18}O$. J. Quant. Spectrosc. Radiat. Transf. 111, 2160–2184.

Tennyson, J., et al., 2013. IUPAC critical evaluation of the rotational–vibrational spectra of water vapor, part III: energy levels and transition wavenumbers for $H_2{}^{16}O$. J. Quant. Spectrosc. Radiat. Transf. 117, 29–58.

Tennyson, J., et al., 2014. IUPAC critical evaluation of the rotational–vibrational spectra of water vapor. Part IV. Energy levels and transition wavenumbers for $D_2{}^{16}O$, $D_2{}^{17}O$, and $D_2{}^{18}O$. J. Quant. Spectrosc. Radiat. Transf. 142, 93–108.

Tinetti, G., Encrenaz, T., Coustenis, A., 2013. Spectroscopy of planetary atmospheres in our galaxy. The Astron. Astrophys. Rev. 21, 63.

Toth, R.A., 1986. Frequencies of N_2O in the 1100- to 1440-cm^{-1} region 1440-cm^{-1} region. J. Opt. Soc. America B: Optical Phys. 3, 1263–1281.

Toth, R.A., Brown, L.R., Miller, C.E., Malathy Devi, V., Benner, D.C., 2008. Spectroscopic database of CO_2 line parameters: 4300-7000 cm^{-1}. J. Quant. Spectrosc. Radiat. Transf. 109, 906–921.

Ulenikov, O.N., Onopenko, G.A., Tyabaeva, N.E., Anttila, R., Alanko, S., Schroderus, J., 2000. Rotational analysis of the ground state and the lowest fundamentals ν_3, ν_5, and ν_6 of $^{13}CH_3D$. J. Mol. Spectrosc. 201, 9–17.

Voronin, B.A., Tennyson, J., Tolchenov, R.N., Lugovskoy, A.A., Yurchenko, S.N., 2010. A high accuracy computed line list for the HDO molecule. Mon. Not. R. Astron. Soc. 402, 492–496.

Watson, J.K.G., 1968. Simplification of the molecular vibration-rotation Hamiltonian. Mol. Phys. 15, 479–490.

Watson, J.K.G., 1988. The asymptotic asymmetric-top rotational partition function. Mol. Phys. 65, 1377–1397.

Young, M.E., Fossati, L., Koskinen, T.T., Salz, M., Cubillos, P.E., France, K., 2020. Non-Local Thermodynamic Equilibrium Transmission Spectrum Modelling of HD 209458b. A&A, p. 641.